Design and synthesis of an RGD peptidomimetic-paclitaxel conjugate targeting $\alpha_v\beta_3$ integrin for tumour-directed drug delivery

Monica Piras,*[a] Alexandra Andriu,[a] Andrea Testa,[a] Paul Wienecke,[a] Ian N. Fleming,[a] Matteo Zanda*[a,b]

[a] Institute of Medical Sciences and Kosterlitz Centre for Therapeutics, School of Medicine, Medical Sciences and Nutrition, University of Aberdeen, Foresterhill, Aberdeen, AB25 2ZD (Scotland, UK).

[b] C.N.R. – I.C.R.M., via Mancinelli 7, 20131 Milan (Italy).

m.zanda@abdn.ac.uk

This article is dedicated to Professor Victor Snieckus on the occasion of his 80th Birthday

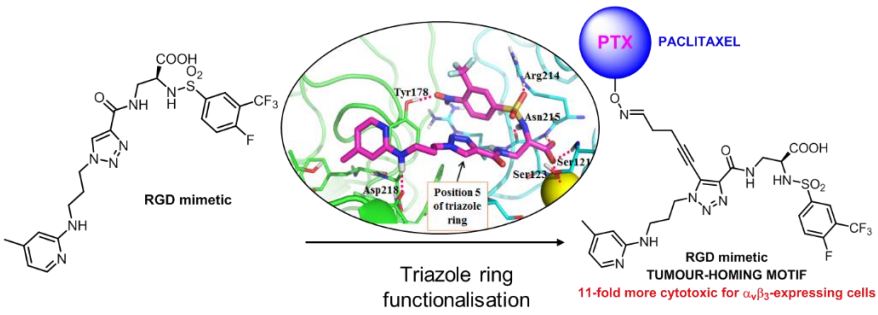

Abstract. A 1,2,3-triazole-based RGD peptidomimetic having nanomolar affinity for $\alpha_v\beta_3$ integrin was conjugated to the potent antimitotic paclitaxel via an oxime heterobifunctional linker. The resulting construct maintained nanomolar binding concentration to $\alpha_v\beta_3$ integrin and showed 11-fold selectivity in terms of cytotoxicity towards highly $\alpha_v\beta_3$ expressing U87MG cancer cells relative to non $\alpha_v\beta_3$ expressing MCF7 cells, indicating promising cancer cell targeting capacity.

Key words RGD, peptidomimetic, integrin, paclitaxel, click, cytotoxicity, cancer

The efficacy of chemotherapeutic agents clinically used for the treatment of malignant tumours is generally limited by their non-specific toxicity against off-target cells, especially those characterised by a high proliferation rate, resulting in a reduced therapeutic index and serious side effects (e.g. alopecia, nausea, vomiting and immunosuppression). Several strategies have been developed over the years in order to overcome these problems and achieve a tumour-targeted delivery of cytotoxic agents.[1] An attractive approach is represented by hybrid compounds, containing a cytotoxic drug bound to a moiety that specifically identifies protein markers overexpressed on cancer cells. Thanks to the development of phage display technologies, several peptide sequences capable of recognising tumour markers have been discovered and extensively investigated as valuable tools for tumour-targeted delivery of chemotherapeutics.[1-2] RGD-containing peptides targeting $\alpha_v\beta_3$ integrin belong to this class of tumour-homing vectors. The overexpression of $\alpha_v\beta_3$ on solid tumours, along with its capacity to be internalised *via* endocytosis after binding of ligands such as RGD peptides, makes it an attractive target for tumour delivery of anticancer agents.[3] A number of cytotoxic drugs have been conjugated to tumour-homing peptides containing the RGD motif and the resulting constructs assessed in animal models. Several studies in this field provided experimental evidence that RGD-based strategies contribute to reduce the toxicity and augment the therapeutic window of existing chemotherapeutics.[1,4,5]

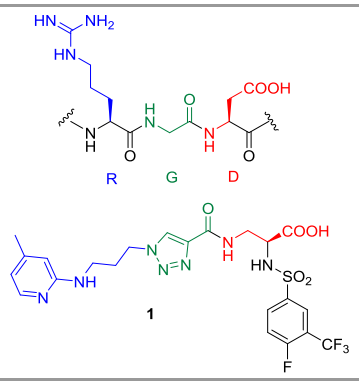

Figure 1. Structure of the RGD parent peptide and a triazole-based RGD peptidomimetic (**1**).[6] The chemical groups mimicking the arginine (R), glycine (G) and aspartate (D) amino acids are coloured in blue, green and red, respectively.

In previous studies we have described the rational design of a new class of integrin ligands based on a triazole scaffold that led to the discovery of RGD peptidomimetics highly active for $\alpha_v\beta_3$ and selective against the platelet receptor $\alpha_{IIb}\beta_3$ (compound 1, Figure 1).[6] Herein, we report the design and synthesis of a 1,2,3-triazole-based RGD peptidomimetic conjugated with the potent antimitotic agent paclitaxel (PTX), and its selectivity (11-fold) towards $\alpha_v\beta_3$ expressing cells relative to PTX alone.

Design. An important feature of RGD-cytotoxic conjugates is that, once internalised into the target cells, they should be promptly disassembled resulting in the release of the cytotoxic agent. Derivatives characterised by an excessive stability could irreversibly impair the therapeutic activity of the parent drug. On the other hand, functionalities that prematurely release the chemotherapeutic agent by metabolic or chemical breakdown, will compromise the targeted delivery strategy resulting in off-target toxicity. Usually, amides, hydrazides, carbamates and sterically hindered esters are used to connect the cytotoxic drug to the tumour-homing moiety through a linker.[4,7] Conjugation of PTX to RGD ligands could be performed *via* cleavable succinyl ester linker attached to the 2′-OH group of PTX (Scheme 1). As the 2′-OH function is essential for PTX to exert its cytotoxic and microtubule-stabilising activities, it should be easily released from the ester function once delivered to the target organ.[8] It has been shown that the succinyl ester bond at the PTX-2′ position is sufficiently stable to guarantee tumour-selective delivery of RGD-PTX conjugates and is enzymatically cleaved *in vivo* by esterases to provide PTX into its active form.[4] While the cytotoxic agent is converted into an inactive prodrug by coupling to an RGD carrier, the RGD-ligand should maintain its capacity to bind the $\alpha_v\beta_3$ receptor when attached to the cytotoxic payload. In this regard, SAR studies conducted on triazole-based RGD mimetics[6] provided essential information for the rational design of active derivatives functionalised with a handle necessary for the ligation of the cytotoxic cargo. We have demonstrated that the functional moieties of this class of ligands mainly responsible for integrin recognition are (i) the carboxylic function, (ii) the sulfonamide group, (iii) the electron withdrawing substituents on the phenyl ring and (iv) the basic 2-aminopyridine (Figure 2). Conversely, the triazole ring, lying at the interface between the α and β subunits, acts as a spacer between the major functional groups involved in ligand-receptor interactions and, therefore, it appears to be the most suitable site for functionalisation. Noteworthy is the fact that incorporation of a bulky substituent - like iodine - in position 5 of the triazole ring did not affect the binding properties of this class of ligands.[6] Taking into account all of these aspects, we designed the construct **3** formed by (i) PTX-2′-succinate, (ii) the RGD mimetic **1** equipped with a chemical handle on the triazole ring and (iii) a heterobifunctional linker **4** connecting these two portions (Scheme 1).

Retrosynthesis. The synthesis of conjugate **3** is based on the convergent assembly of three building blocks (Scheme 1): (i) the PTX-2′-succinate activated as *N*-hydroxysuccinimide (NHS) ester **2**, (ii) the RGD ligand functionalised with a chemical handle bearing an aldehyde function **5** and (iii) the heterobifunctional linker 4-(aminooxy)butan-1-amine **4**. Based on our retrosynthetic plan (Scheme 1), the aldehyde **5** can be generated by oxidation of the key intermediate alcohol **6** obtained connecting the iodinated precursor **7** and 4-pentynol **8** *via* Sonogashira cross-coupling (Scheme 1).

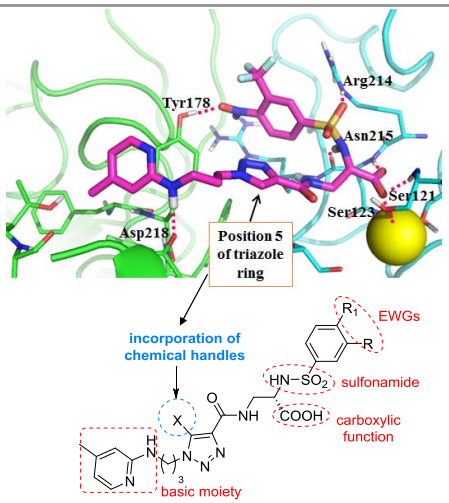

Figure 2. Predicted binding mode of triazole-based RGD peptidomimetics on integrin $\alpha_v\beta_3$ (top).[6] The functional groups involved in the ligand-receptor recognition process are circled in red (bottom). The position 5 of the triazole ring (blue circle) has been selected as a suitable position for the attachment of the cytotoxic payload.

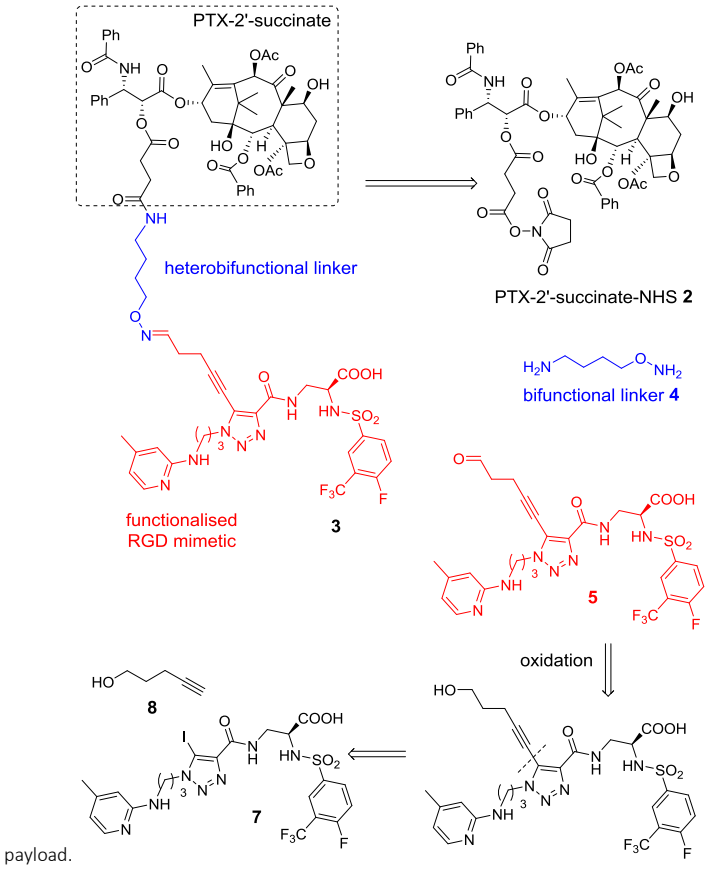

Scheme 1. Retrosynthetic approach to the target conjugate **3**.

Synthesis. For the synthesis of the building block PTX-2′-succinate-NHS ester **2** (Scheme 1), the 2′-hydroxyl function of PTX was derivatised with succinic anhydride following a procedure reported in literature.[9] The resulting PTX-succinate was activated as NHS ester **2** using *N*,*N*′-dicyclohexylcarbodiimide (DCC) as coupling reagent, as already described.[9]

The key RGD intermediate **6** (Scheme 2) was synthesised *via* Sonogashira cross-coupling between the iodinated precursor **7** and 4-pentyn-1-ol **8**. A number of conditions were explored (Table 1). Application of typical Sonogashira protocol on this substrate (phosphine-ligated Pd catalyst, CuI as co-catalyst and an amine as a base)[10] afforded no reaction at room temperature and decomposition at higher temperatures (entries 1–4). Similarly, following a ligand-

, copper- and amine- free strategy reported by Urgaonkar and Verkade, based on the use of Pd acetate ($Pd(OAc)_2$) and tetrabutylammonium acetate (Bu_4NOAc) as a base,[11] no reaction was observed at r.t. (entry 5). By increasing the temperature no decomposition occurred, although only starting material was recovered (entry 6). Addition of TEA to $Pd(OAc)_2$ and Bu_4NOAc gave rise to the formation of trace amounts of **6** at 60 °C after 6 hours (entry 7). Using TEA (3 equiv) and a large excess of alkyne (10 equiv) the desired alkynylated product **6** was eventually obtained in good yields (70%) in less than 6 hours (entry 8).[12]

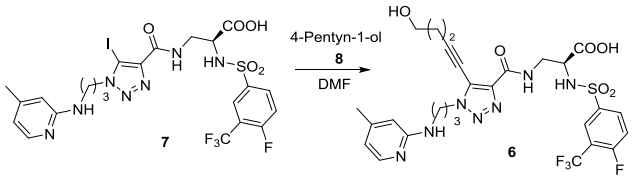

Scheme 2. Synthesis of **6** *via* Sonogashira cross-coupling.

Table 1. Reaction conditions tested for Sonogashira cross-coupling

Entry	Catalyst	8 (equiv)	Temp (h)	base	Time	Yield[a]
1	$Pd(PPh_3)_4$+CuI	1	25	TEA	12	NR
2	$Pd(PPh_3)_4$+CuI	1	60	TEA	6	D
3	$Pd(PPh_3)_2Cl_2$+CuI	1	25	TEA	12	NR
4	$Pd(PPh_3)_2Cl_2$+CuI	1	60	TEA	6	D
5	$Pd(OAc)_2$	1.25	25	Bu_4NOAc	12	NR
6	$Pd(OAc)_2$	1.25	60	Bu_4NOAc	12	NR
7	$Pd(OAc)_2$	1.25	60	Bu_4NOAc +TEA	6	low yield
8	$Pd(OAc)_2$	10	60	Bu_4NOAc +TEA	12	70 %

[a]The reaction course was monitored via RP-HPLC coupled to tandem ESI-MS.
NR = no reaction, starting material recovered; D = decomposition

The heterobifunctional linker **4** (Scheme 3) was synthesised starting from 1-bromo-4-cloro butane **9** that, reacting with sodium azide at room temperature in DMF, afforded 1-cloro-4-azido butane **10**. Treatment of **10** with *N*-Boc protected hydroxylamine in the presence of a base led to the formation of **11**, which was converted into the amino derivative **12** by Staudinger reaction. *N*-Boc cleavage of **12** with TFA afforded the final product **4** in good overall yields. The assembly of the conjugate **3** was straightforward (Scheme 4). Conversion of alcohol **6** into aldehyde **5** was performed under mild conditions using Dess-Martin periodinane (DMP) reagent. The reaction was monitored by RP-HPLC coupled to tandem ESI-MS. After total consumption of the starting material **6**, the heterobifunctional linker **4** was added to the same reaction flask generating the intermediate **13** *via* chemoselective oxime bond formation.[13] Purification of **13** was performed by semipreparative RP-HPLC. The free amino function of **13** was then reacted with PTX-2′-succinate-NHS ester **2** in the presence of DIPEA to provide the final conjugate **3** in 54% yield after chromatographic purification.

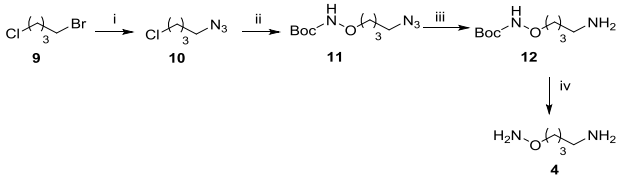

Scheme 3. Synthesis of 4. *Reagents and conditions*: (i) NaN_3, DMF, room temp, overnight, 99%; (ii) BocNHOH, DBU, DMF, room temp, 2h, 40%; (iii) PPh_3, THF, room temp, 1h then H_2O, 60 °C, 4h, 99%; (iv) TFA-CH_2Cl_2 (1:1), rt, 2h, 99%.

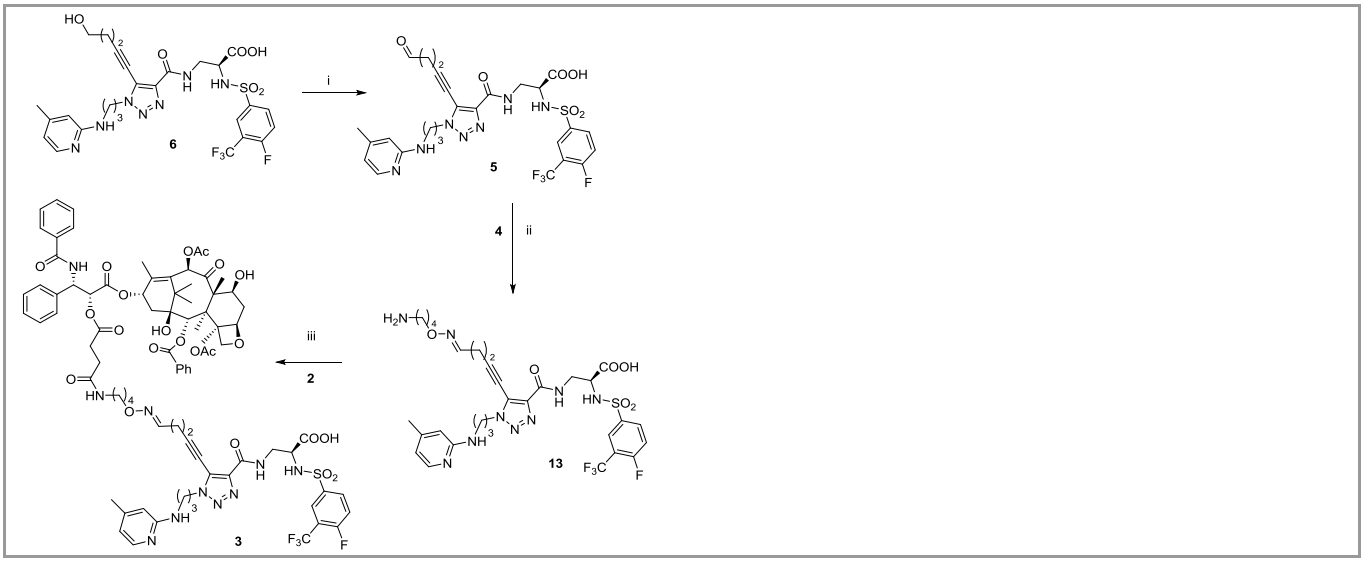

Scheme 4. Synthesis of **3**. *Reagents and conditions*: (i) DMP, CH_3CN, room temp, 6h, then (ii) **4**, room temp, 1h, 60%; (iii) DIPEA, DMF, room temp, 5h, 54%.

Solid-phase receptor binding assay. The RGD mimetic **6** functionalised with a chemical handle and the conjugate construct **3** were submitted to biological assays to measure their affinity for the $\alpha_v\beta_3$ receptor. Competitive affinities were calculated analysing the interactions between immobilised $\alpha_v\beta_3$ and the commercially available *c*[RGDfK(Biotin-PEG-PEG)] peptide in the presence of increasing amounts of ligands, as already described.[15] The IC_{50} values of **6** and **3** were compared to that of the non-functionalised peptidomimetic **1** and the $\alpha_v\beta_3$-inhibitor *c*(RGDfK) (Table 2). Notably, functionalisation of the highly active RGD mimetic **1** with an alkynyl chemical handle to give the derivative **6** was performed without perturbing the binding affinity of the parent ligand (Table 2, entries 2 and 3). Conversely, the large increase of steric hindrance in the conjugate **3** caused a ~10-fold drop in binding affinity (Table 2, entries 2 and 4). However, the IC_{50} value of **3** was still in the nanomolar range and not significantly different from that of the reference *c*(RGDfK) peptide used as positive control (Table 2, entries 1 and 4).

Table 2 Inhibition of cyclo[RGDfK(Biotin-PEG-PEG)] binding to immobilised $\alpha_v\beta_3$.

entry	compound	IC_{50} (nM)[a]
1	***c*(RGDfK)**	138 ± 51
2	**1**	25 ± 3
3	**6**	20 ± 1
4	**3**	200 ± 46

[a]Data are the average of two independent experiments performed in triplicate; standard deviations are shown

Cell cytotoxicity assays. Conjugate **3** was tested *in vitro* to assess its cytotoxicity towards MCF7 and U87MG tumour cells, which express no and high levels of $\alpha_v\beta_3$ integrin, respectively. The unconjugated ligand **1** and free PTX were also included in the study. In order to reliably assess the selective cytotoxicity of conjugate **3** against $\alpha_v\beta_3$ positive cell lines, a "cell washout" cytotoxicity assay was performed.[16] Following this procedure - aimed at mimicking the in vivo conditions where the administered drug is rapidly cleared from the extracellular tumour environment - cells were incubated with the cytotoxic agents for a short period of time (6 h) and then the medium was washed away to remove the non-internalised conjugate **3**. Using this method, the possible anti-proliferative activity arising from extracellular cleavage of the linker from **3 -** and consequent undesired drug release - can be minimised.[17] As expected, cytotoxicity assays clearly indicated that the tumour-homing peptidomimetic **1** was not cytotoxic (Table 3) when used at concentrations up to 10,000 nM. In contrast, PTX was potently cytotoxic to both cell lines, as a result of its capacity to readily enter the cells and inhibit microtubule disassembly. Conjugate **3** was also cytotoxic for both cell lines, although IC_{50} values were considerably higher than for PTX, indicating that the construct was not hydrolysed and did not release free PTX during incubation.

Table 3 Cell sensitivity of U87MG and MCF7 tumour cells to PTX, **3** and **1**

Cell line	**Compound 1 IC_{50} (nM)[a]**	**Compound 3 IC_{50} (nM)[a]**	**PTX IC_{50} (nM)[a]**

MCF7 ($\alpha_v\beta_3$-)	> 10, 000	*$21.6 \cdot 10^3 \pm 10.6 \cdot 10^3$*	*41.3 ± 14*
U87MG ($\alpha_v\beta_3$++)	> 10, 000	*$1.99 \cdot 10^3 \pm 1.59 \cdot 10^3$*	*44.4 ± 26*
Selectivity[c]	-	*11*	*1.0*

[a] IC_{50} values were calculated as the concentration of compound required for 50% inhibition of cell viability in culture. The number of cells in each well was measured using an (3-(4,5-dimethylthiazol-2-yl)-2,5-diphenyltetrazolium bromide (MTT) cell proliferation assay, as described [ref. 18];
[b]Cytotoxicity ratio for U87MG vs MCF7 is statistically significant; (p value <0.01 in one way ANOVA). Compound **1** exhibited no significant cytotoxicity when tested at concentrations up 10,000 nM.
[c] Selectivity: $IC_{50}(\alpha_v\beta_3-)/IC_{50}(\alpha_v\beta_3++)$.

As expected, PTX was not $\alpha_v\beta_3$-selective, showing essentially the same IC_{50} on both highly $\alpha_v\beta_3$ integrin expressing cells (U87MG) and non-expressing cells (MCF7). In contrast, the conjugate **3** showed good selectivity index = 11 (determined by the IC_{50}(MCF7)/IC_{50}(U87MG) ratio), indicating a higher cytotoxicity for U87MG vs. MCF7 cells. This is consistent with the hypothesis that compound **3** can selectively target cancer cells via $\alpha_v\beta_3$ integrin.

Metabolic stability assays.[19] The conjugate **3** and the RGD mimetic **1** were subjected to human and rat liver microsomal stability tests to determine *in vitro* their stability towards cytochrome P (CYP)-mediated metabolism. Test compounds were incubated with rat and human microsomes at 37 °C in the presence of the co-factor NADPH. The reaction was terminated by the addition of methanol. Following centrifugation, the supernatant was analysed on the LC-MS/MS. From this study emerged that both the tumour-homing moiety **1** and the cytotoxic construct **3** were considerably stable both in human and rat microsome suspensions (half-life 770 and 470 min, respectively). The fate of the conjugate **3** upon incubation with U87MG cells was also investigated. HPLC/MS analysis and ^{19}F NMR spectroscopy of both cell lysate and culture medium confirmed that after 24 hours the conjugate **3** is still present unchanged, whereas a minor HPLC peak corresponding to free PTX could also be detected. This confirm the substantial stability of **3** and the slow release of PTX in the presence of cells,

Conclusions. In this work, we described the rational design of a novel tumour-targeted cytotoxic conjugate **3** incorporating the potent antimitotic paclitaxel (PTX). The triazole-based RGD mimetic **1** was designed as the tumour-homing motif of the chemotherapeutic construct. The targeting vector **1** was then functionalised with a chemical handle on the triazole ring, which was identified as the most suitable site for derivatisation of the RGD mimetic scaffold. Measurement of the binding affinity of the functionalised mimetic **6** demonstrated that the alkynyl chain on the triazole ring did not affect the high affinity of **1** for $\alpha_v\beta_3$ integrin. The synthesis of the conjugate **3** was performed by linking the cytotoxic agent **2** and the RGD carrier **5** through a heterobifunctional linker **4**. The strong increase of steric hindrance in the construct **3** caused a ~10-fold drop in binding affinity, however, the IC_{50} value of **3** remained in the nanomolar range and was not significantly different relative to that of the reference *c*(RGDfK) peptide. PTX and conjugate **3** were then tested *in vitro* to assess their cytotoxic activity towards MCF7 and U87MG tumour cells, which express no and high levels of $\alpha_v\beta_3$ integrin, respectively, using a "cell washout" assay. Under these conditions, PTX was found to be cytotoxic on both cell lines irrespectively of their $\alpha_v\beta_3$ integrin-expression level, while the cytotoxic activity of conjugate **3** was dependent on $\alpha_v\beta_3$ integrin expression. These results demonstrate the capacity of **3** to selectively deliver the cytotoxic paclitaxel cargo through $\alpha_v\beta_3$ integrin interaction. *In vitro* human and rat liver microsomal stability tests showed a remarkable stability of both conjugate **3** and RGD carrier **1** against CYP-mediated hepatic metabolism. Further studies will be performed in the future to assess the *in vivo* capacity of the conjugate **3** to increase the therapeutic window and limit the peripheral toxicity of PTX.

Acknowledgment

We thank the Development Trust, University of Aberdeen, for funding a fellowship to M.P. and a studentship to A.A.

Supporting Information

See the accompanying file.

References and Notes

(1) Svensen, N.; Walton, J. G.; Bradley, M. *Trends Pharmacol. Sci.* **2012**, *33*, 186.
(2) Arap, W.; Pasqualini, R.; Ruoslahti, E. *Science* **1998**, *279*, 377.
(3) Chen, K.; Chen, X. *Theranostics* **2011**, *1*, 189.
(4) Colombo, R.; Mingozzi, M.; Belvisi, L.; Arosio, D.; Piarulli, U.; Carenini, N.; Perego, P.; Zaffaroni, N.; De Cesare, M.; Castiglioni, V.; Scanziani, E. *J. Med. Chem* **2012**, *55*, 10460.
(5) Liu, Y.; Bajjuri, K. M.; Liu, C.; Sinha, S.C. *Mol. Pharm.* **2012**, *9*, 168.

(6) Piras, M.; Testa, A.; Fleming, I. N.; Dall'Angelo, S.; Andriu. A.: Menta. S.: Mori. M.; Brown, G. D.; Forster, D.; Williams, K. J.; Zanda, M. *ChemMedChem* **2017,** in press, DOI: 10.1002/CMDC.201700328.
(7) Dal Pozzo, A.; Ni, M. H.; Esposito, E.; Dallavalle, S.; Musso, L.; Bargiotti, A.; Pisano, C.; Vesci, L.; Bucci, F.; Castorina, M.; Foderà, R. *Bioorg. Med. Chem.* **2010**, *18*, 64.
(8) Fu, Y.; Li, S.; Zu, Y.; Yang, G.; Yang, Z.; Luo, M.; Jiang, S.; Wink, M.; Efferth, T. *Curr. Med. Chem.* **2009**, *16*, 3966.
(9) Gao, Y.; Kuang, Y.; Guo, Z.F.; Guo, Z.; Krauss, I.J.; Xu, B. *J. Am. Chem. Soc.* **2009**, *131*, 13576.
(10) Chinchilla, R.; Nájera, C. *Chem. Soc. Rev.* **2011**, *40*, 5084.
(11) Urgaonkar, S.; Verkade, J.G. *J. Org. Chem.* **2004**, *69*, 5752.
(12) Synthesis of **6**. To a solution of **7** (as TFA salt, 22 μmol, 20 mg, 1 equiv) in dry DMF (500 μL) TEA (66 μmol mmol, 10 μL, 3 equiv), *n*-Bu_4NOAc (66 μmol, 20 mg, 3 equiv), a catalytic amount of $Pd(OAc)_2$ and alkyne **8** (0.22 mmol, 18 mg, 10 equiv) were added. The reaction was stirred at 60 °C for 6 h. The mixture was cooled to r.t., diluted with water (4 mL) and then filtered using a 0.20 μm syringe filter. The filtrate was purified by semi-preparative RP-HPLC. Analytical RP-HPLC conditions (solvent A = H_2O + 0.1% TFA, solvent B = CH_3CN, gradient: from 30% B to 50% B in 15 min; flow: 1 mL/min; R_t = 7 min). The product was lyophilized affording 12 mg of a yellow solid (70% yield, isolated as TFA salt): ^{1}H NMR (400 MHz, CD_3OD) δ 8.21 – 8.05 (m, 2H), 7.73 (d, *J* = 6.6 Hz, 1H), 7.51 – 7.37 (m, 1H), 6.85 (s, 1H), 6.80 (dd, *J* = 6.7, 1.4 Hz, 1H), 4.62 (t, *J* = 6.6 Hz, 2H), 4.29 (dd, *J* = 8.9, 4.9 Hz, 1H), 3.82 (dd, *J* = 13.8, 4.9 Hz, 1H), 3.74 (t, *J* = 6.1 Hz, 2H), 3.52 (dd, *J* = 13.8, 8.9 Hz, 1H), 3.42 (t, *J* = 6.7 Hz, 2H), 2.68 (t, *J* = 7.0 Hz, 2H), 2.43 (s, 3H), 2.41 – 2.29 (m, 2H), 1.93 – 1.83 (m, 2H); ^{19}F NMR (376 MHz, CD_3OD) δ −63.15 (d, *J* = 12.7 Hz), −76.96 (s), −110.64 (q, *J* = 12.7 Hz); ^{13}C NMR (101 MHz, CD_3OD) δ 170.9, 161.4 (d, *J* = 261.5 Hz), 160.4, 156.7, 152.7, 141.4, 138.2 (d, *J* = 3.7 Hz) , 134.2, 133.6 (d, *J* = 10.3 Hz), 126.3, 122.8, 121.9 (q, *J* = 271.4 Hz), 117.7 (d, *J* = 22.2 Hz), 114.5, 111.6, 106.2, 64.6, 60.0, 55.4, 45.9, 40.7, 38.6, 30.3, 27.5, 20.5, 15.7; MS (ESI, *m/z*): calculated for $C_{27}H_{30}F_4N_7O_6S$ $[M+H]^+$ 655.18 found 655.2.
(13) Synthesis of **13**. To a suspension of **6** (65 μmol, 50 mg, 1 equiv) and DMP (97.5 μmol, 41 mg, 1.5 equiv) in CH_3CN (1 mL) DMSO was added dropwise until the solution became clear. The mixture was stirred at r.t. for 6 h and then filtered to remove a white precipitate formed during the reaction. To the filtered solution **4** (195 μmol, 25 mg, 3 equiv) was added and the mixture was stirred for 1 h at r.t. The product was purified by semi-preparative RP-HPLC. Analytical RP-HPLC conditions (solvent A = H_2O + 0.1% TFA, solvent B = CH_3CN, gradient: from 30% B to 50% B in 15 min; flow: 1 mL/min; R_t: 4.8 min). The product was lyophilized affording 38 mg of a pale yellow solid (60% yield, isolated as bis TFA salt) containing a mixture of oxime E/Z isomers (3:2). Minor isomer resonances are denoted by an asterisk*: ^{1}H NMR (400 MHz, CD_3OD) δ 8.08 – 8.00 (m, 2H), 7.63 (d, *J* = 6.2 Hz, 1H), 7.49 (t, *J* = 5.7 Hz, 0.6H), 7.38 – 7.28 (m, 1H), 6.80* (t, *J* = 5.1 Hz, 0.4H), 6.69 (s, 1H), 6.65 (d, *J* = 6.1 Hz, 1H), 4.50 (t, *J* = 6.3 Hz, 2H), 4.10 – 3.92 (m, 3H), 3.78 – 3.62 (m, 1H), 3.48 – 3.34 (m, 1H), 3.30 (t, *J* = 6.1 Hz, 2H), 2.91 – 2.79 (m, 2H), 2.67 (t, *J* = 6.8 Hz, 2H), 2.62 – 2.53 (m, 1H), 2.43 (m, 1H), 2.29 (s, 3H), 2.27 – 2.17 (m, 2H), 1.72 – 1.57 (m, 4H); ^{19}F NMR (376 MHz, CD_3OD) δ −63.10 (d, *J* = 12.7 Hz), −76.95, −110.39 – −110.82 (m); MS (ESI, *m/z*): calculated for $C_{31}H_{38}F_4N_9O_6S$ $[M+H]^+$ 740.25 found 740.2.
(14) Synthesis of **3**. To a solution of PTX-2′-succinate-NHS ester **2** (24 μmol, 25 mg, 1 equiv) in DMF (0.5 mL) at rt., DIPEA (72 μmol, 13 μL, 3 equiv) and **13** (24 μmol, 23 mg, 1 equiv) were added. The reaction mixture was stirred for 5 h at r.t., then filtered and purified by semi-preparative RP-HPLC. Analytical RP-HPLC conditions (solvent A = H_2O + 0.1% TFA, solvent B = CH_3CN, gradient: from 50% B to 1000% B in 15 min, flow: 1 mL/min; R_t: 6.9 min). The product was lyophilized affording 23 mg of a white solid (54% yield, isolated as TFA salt) containing a mixture of oxime E/Z isomers (3:2). Minor isomer resonances are denoted by an asterisk*: ^{1}H NMR (400 MHz, CD_3OD) δ 9.03 (d, *J* = 8.7 Hz, 1H), 8.29 – 8.20 (m, 1H), 8.05 – 7.98 (m, 4H), 7.76 – 7.70 (m, 2H), 7.62 – 7.55 (m, 2H), 7.55 – 7.26 (m, 11H), 7.15 (t, *J* = 7.1 Hz, 1H), 6.78* (t, *J* = 5.1 Hz, 0.4H), 6.73 (s, 1H), 6.67 (dd, *J* = 6.6, 1.3 Hz, 1H), 6.33 (s, 1H), 5.94 (t, *J* = 9.0 Hz, 1H), 5.68 (d, *J* = 6.6 Hz, 1H), 5.52 (d, *J* = 7.2 Hz, 1H), 5.33 (dd, *J* = 6.7, 1.2 Hz, 1H), 4.88 (d, *J* = 8.1 Hz, 1H), 4.48 (t, *J* = 6.0 Hz, 2H), 4.31 – 4.13 (m, 2H), 4.07 (s, 2H), 3.96 (t, *J* = 6.3 Hz, 1H), 3.89 (t, *J* = 6.3 Hz, 1H), 3.76 – 3.66 (m, 2H), 3.60 – 3.45 (m, 1H), 3.45 – 3.35 (m, 1H), 3.34 – 3.25 (m, 2H), 3.09 – 2.97 (m, 2H), 2.72 – 2.53 (m, 5H), 2.48 – 2.34 (m, 4H), 2.33 – 2.19 (m, 8H), 2.10 – 1.97 (m, 4H), 1.80 (s, 3H), 1.75 – 1.60 (m, 2H), 1.60 – 1.37 (m, 8H), 1.03 (s, 3H), 1.02 (s, 3H); ^{19}F NMR (376 MHz, CD_3OD) δ −63.06* (d, *J* = 12.7 Hz), −63.07 (d, *J* = 12.7 Hz), −77.19 (s), −110.47 – −110.61 (m); ^{13}C NMR (101 MHz, CD_3OD) δ 203.8, 172.4, 172.2, 170.8, 170.1, 169.9, 169.1, 169.0, 166.2, 161.4 (d, *J* = 260.6 Hz), 160.3, 152.6, 149.3*, 148.6, 141.7, 141.6, 141.0, 138.1 (d, *J* = 3.7 Hz), 137.0, 134.2, 134.1, 133.6 (d, *J* = 9.9 Hz), 133.4, 133.2, 131.5, 129.9, 129.8, 128.7, 128.3, 128.1, 127.2, 127.2, 122.5 (d, *J* = 2.8 Hz), 121.9 (q, *J* = 272.6 Hz), 117.7 (d, *J* = 22.1 Hz), 114.6, 105.1, 84.4, 80.8, 78.0, 77.6, 76.0, 75.3, 74.6, 73.2, 72.7, 71.4, 70.9, 70.0, 65.3, 65.2, 57.8, 55.3, 54.0, 46.4, 45.9, 43.1, 40.7, 38.8, 38.6, 36.0, 34.9, 29.8, 29.3, 28.6, 27.7, 27.5, 26.1, 26.0, 25.5, 25.5, 23.9, 21.8, 20.9, 20.6, 19.4, 16.7, 16.2, 13.6, 9.0; MS (ESI, *m/z*): calculated for $C_{82}H_{91}F_4N_{10}O_{22}S$ $[M+H]^+$ 1675.59 found 1675.7.
(15) Piras, M.; Fleming, I. N.; Harrison, W. T.; Zanda, M. *Synlett* **2012**, *23*, 2899.
(16) Dal Corso, A.; Caruso, M.; Belvisi, L.; Arosio, D.; Piarulli, U.; Albanese, C.; Gasparri, F.; Marsiglio, A.; Sola, F.; Troiani, S.; Valsasina, B. *Chem. Eur. J.* **2015**, *21*, 6921.
(17) Cell cytotoxic assay:
Cells were seeded in 96-well plates at either 2,500 cells/well (MCF7 cells) or 4,000 cells/well (U87MG cells) and left to grow for 48 h in RPMI containing 10 % foetal calf serum (FCS). Stock solutions of compound **1**, **3** and paclitaxel (PTX) were prepared in DMSO and diluted to test concentrations in RPMI containing 10 % FCS. Cells were exposed to a range of concentrations of test compound for 6 hours in triplicate wells. Medium containing the compounds was then removed by aspiration and replaced with fresh RPMI containing 10% FCS. Cells were left to grow for 72 h. The number of cells in each well was then measured using an (3-(4,5-dimethylthiazol-2-yl)-2,5-diphenyltetrazolium bromide (MTT) cell proliferation assay. Cells convert the MTT reagent into formazan which can be detected at 562 nm in a microplate reader. The concentration of each compound that inhibits cell proliferation by 50% (IC_{50}) was calculated using Graph PAD PRISM. In addition, for each experiment a selectivity ratio was calculated for compound **3** by dividing the IC_{50} for compound **3** with the paclitaxel IC_{50}.

Each IC_{50} value and ratio is the average ± s.e. of 4 independent experiments. A one way ANOVA was performed using IBM SPSS Statistics version 24, to compare the selectivity ratios obtained in the different cell lines.
(18) Lamidi, O.F.; Sani, M.; Lazzari, P.; Zanda, M.; Fleming, I.N. *J. Cancer Res. Clin. Oncol.* **2015**, *141*, 1575.
(19) In vitro stability assays:
All assays conducted by Cyprotex Ltd (Macclesfield, UK).
Human and rat liver microsomal stability assays: Briefly: Test compound (3 μM) was incubated with pooled liver microsomes. Test compound was incubated at 5 time points over the course of a 45 min experiment and the test compound was analysed by LC-MS/MS. Experimental Procedure: pooled human or mouse liver microsomes were purchased from a reputable commercial supplier. Microsomes were stored at -80 °C prior to use. Microsomes (final protein concentration 0.5 mg/mL), 0.1 M phosphate buffer pH 7.4 and test compound (final substrate concentration 3 μM; final DMSO concentration 0.25 %) were pre-incubated at 37 °C prior to the addition of NADPH (final concentration 1 mM) to initiate the reaction. The final incubation volume was 50 μL. A minus cofactor control incubation was included for each compound tested where 0.1 M phosphate buffer pH 7.4 was added instead of NADPH (minus NADPH). Two control compounds were included with each species. All incubations were performed singularly for each test compound. Each compound was incubated for 0, 5, 15, 30 and 45 min. The control (minus NADPH) was incubated for 45 min only. The reactions were stopped by transferring 20 μL of incubate to 60 μL methanol at the appropriate time points. The termination plates were centrifuged at 2,500 rpm for 20 min at 4 °C to precipitate the protein. Quantitative Analysis: following protein precipitation, the sample supernatants were combined in cassettes of up to 4 compounds, internal standard was added and samples analysed using Cyprotex generic LC-MS/MS conditions.